Journal of Applied Mathematics and Physics, 2022, 10, 1509-1524
https://www.scirp.org/journal/jamp
ISSN Online: 2327-4379
ISSN Print: 2327-4352

Mechanical Analysis of Interface in Coating Structure under Conical Concave Indenter with FEM

Shi-Qing Huang[1,2*], Pan-Jun Tang[1,2*], Wen-Hua Zhang[1,2#]

[1]MOE Key Lab of Disaster Forecast and Control in Engineering, Jinan University, Guangzhou, China
[2]School of Mechanics and Construction Engineering, Jinan University, Guangzhou, China
Email: #zwhdwy@hnu.edu.com

How to cite this paper: Huang, S.-Q., Tang, P.-J. and Zhang, W.-H. (2022) Mechanical Analysis of Interface in Coating Structure under Conical Concave Indenter with FEM. *Journal of Applied Mathematics and Physics*, **10**, 1509-1524.
https://doi.org/10.4236/jamp.2022.105106

Received: April 22, 2022
Accepted: May 13, 2022
Published: May 16, 2022

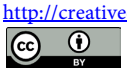

Abstract

The evaluation of mechanical properties of coating structures has always been a very important topic in the fields of mechanics, materials, and machinery. The traditional evaluation methods are easy to produce deviation, because the ratio of coating thickness to substrate thickness is too small. Therefore, accurate analysis and calculation is particularly important. Indentation technology is an important means of coating structure analysis and measurement, the basis of standardized application and analysis of coating structure, and a classical method for accurate analysis and calculation of coating structure. The finite element method is a very good means to analyze and study this kind of problems because of its applicability. Based on the finite element method, this paper analyzes and studies the interface connection form, substrate, and local delamination effects of the indentation behavior of the coating structure under the conical concave indenter. In this paper, the finite element method, which is more convenient for analysis and calculation, is used to analyze the influence of interface connection form, substrate, and local delamination on the coating structure. The results of force displacement, interface normal stress, and interface shear stress are analyzed in detail, and the effects of the three effects on the coating structure are proved. The significance of this study is reflected in: based on the analysis of the three effects of interface connection form, substrate, and local delamination, the mechanical properties of the coating structure are more in-depth, which provides some reference for mechanical engineers to design and test the coating structure.

Keywords

Coating Structure, Finite Element Method, Contact Mechanics, Interfacial

*Both Shi-Qing Huang and Pan-Jun Tang are first authors.

Connection Form Effect, Substrate Effect, Local Delamination Effect

1. Introduction

Coating is a solid continuous film obtained by one-time coating, which is widely used to improve the reliability and durability of structures [1] [2], especially to improve wear [3], corrosion [4] [5] [6] [7] [8], and heat resistance [9] [10] near the surface. The test and characterization of mechanical properties is an important part of coating structure design/inspection, and it is the basis of coating technology improvement [7] [11] [12]. The indentation technique is a very good means to characterize the mechanical properties of the coating structure [13] [14]. The finite element method, as a method with strong applicability [15] [16], can analyze the indentation behavior of the coating structure. Vasiliev *et al.* [17] analyzed the transversely isotropic electroelastic functionally graded piezoelectric conductive conical indenter in detail using indentation technique, and found that the existence of the coating is sufficient to change the contact characteristics. Schwarzer *et al.* [18] discussed the effectiveness of the complete analysis method of elastic normal load and tangential Hertz load of coating substrate composites through the finite element calculation of spherical/plane stress indentation model. The research of many scholars has promoted the development of indentation technology of coating structure.

During the development of coating structure indentation technology, the influence of different effects on coating structure has been studied to varying degrees. Regarding the interfacial connection form effect: 1) Huang *et al.* [19] conducted finite element nanoindentation simulations under three different interfacial friction contact conditions. Through the study of the simulated data, it is concluded that the displacement response of the indenter force and the coating/substrate frictional contact model is consistent with the response of the coating/substrate perfect combination model for increasing the value of friction coefficient. 2) Peng *et al.* [20] investigated the nanoindentation of aluminum (Al) coatings on silicon (Si) substrates by 3D molecular dynamics (MD) simulations. The coating/substrate system is modeled by employing the Lennard-Jones (LJ) potential, a form of interfacial connection that simulates van der Waals forces, to describe the interactions at the coating-substrate interface. 3) Liu *et al.* [21] used the finite element method to analyze the delamination induced by the indentation of the coating-substrate structure, and used the critical tensile stress as the criterion to determine the delamination at the interface between the coating and the substrate. The simulation results show that the delamination depends on the interfacial friction of sliding on the interface. The largest delamination in this coating substrate structure model occurs when the friction coefficient is 0.5. For friction coefficients greater than 0.5, the size of the delaminated region decreases with increasing friction coefficient.

Regarding the substrate effect: 1) The study of Xu *et al.* [22] shows that there

is no universal critical indentation depth, and the substrate effect will be affected when it is exceeded. The critical indentation depth depends on the combination of the coating and the substrate, and is more sensitive to the difference in elastic properties than to the difference in plastic properties of the coating/substrate system. 2) Gamonpilas *et al.* [23] studied the indentation behavior of various coating systems. For all kinds of general coating-substrate systems, the ratio of critical indentation depth to coating thickness is determined, in which the influence of substrate material on the indentation response of coating system is negligible (when the substrate effect can be ignored). The ratio is based on the yield strength and Young's modulus of the coating and substrate. 3) Wang *et al.* [24] analyzed the substrate effect. The indentation response under medium penetration depth to film thickness ratio is given in the numerical results, and the dimensionless equations between the maximum indentation load, the loading curve index and the elastic parameters of the coating/substrate system are established by a large number of finite element simulations.

Regarding the local delamination effect of the interface: 1) Abdul-Baqi *et al.* [25] found that delamination occurs in a tangential mode rather than a normal mode, and begins at two to three times the contact radius. It is also shown that the higher the interface strength is, the higher the initial propagation velocity of the delamination is and the lower the steady velocity is. 2) Diao *et al.* [26] obtained a local delamination diagram for the identification of local delamination of hard coatings, which is a function of the shear strength ratio of coating to substrate and the ratio of coating thickness to half-contact width. 3) Xiao *et al.* [27] studied the mechanism of indentation-induced coating cracking and interfacial delamination in a typical weakly bonded brittle thin coating-substrate system (diamond-like carbon coating with low adhesion on steel substrate) by finite element method. The bilinear bond zone model with specified bond strength and cohesion energy is used to simulate the evolution process of crack and delamination. The effects of bonding zone, elastic modulus and thickness of coating on the indentation response were studied.

From the studies of the above scholars, we can see that the three effects of interface connection form, substrate, and interface local delamination are worth studying. The idea of this paper is based on the finite element method to study the interface connection form, substrate, and interface local delamination of the coating structure under the conical concave indenter. At the same time, the finite element method used in this paper can not only ensure a certain accuracy, but also be very convenient to solve the mechanical properties of the coating structure in complex situations, and facilitate the systematic analysis of the coating structure and check with the new theory developed in the future.

In Section 2, the establishment of contact pair of finite element method is introduced, including the setting of target and contact surfaces (element type) and common real constant, because it is very important to the convergence and accuracy of calculation. In Section 3, different finite element models of coating

structure are set up to simulate different interface connection forms and substrate conditions, and the force displacement results are analyzed in detail. In Section 4, the contact of the finite element method is used to set the delamination area, and the non-delamination area is perfectly fixed between the coating and the substrate. By presupposing that the coating has local delamination at the interface, the finite element models of many kinds of interface local delamination coating structure are calculated and analyzed, and the interface stress of different interface local delamination coating structure and non-delamination coating structure is compared and analyzed.

2. Contact Pair Establishment

The most important thing in the realization of the local delamination of different interface connections and the local delamination of the interface in different regions is to establish contact pairs. The finite element method uses contact elements to simulate contact problems. The contact element is a layer of elements covering the contact surface of the analytical model, which can track the contact position, ensure contact coordination (prevent contact surfaces from penetrating each other), and transfer contact stress (normal stress and friction) between contact surfaces.

Three different elements can be used to simulate in the finite element method: surface-surface contact elements, point-surface contact elements, and point-point contact elements. The coating structure model under the conical concave indenter adopts the element type of surface-surface contact. In the surface-surface contact, the target surface and contact surface (element type), contact algorithm, common real constants, etc. need to be determined.

2.1. Target and Contact Surfaces (Element Types)

Contact problems fall into two broad categories: rigid-soft contact and soft-soft contact. In rigid-soft contact, one surface is completely rigid without strain, stress, and deformation except for rigid body motion, and the other surface is composed of deformable soft material. Soft-to-soft contact is the more common type of contact, where both (or all) contact bodies are deformable (that is, they have similar stiffness).

One surface is designated as the target surface and the other surface is designated as the contact surface, which together are called a contact pair. Contact elements are constrained from intruding into the target surface, whereas target elements can intrude into the contact surface. The contact type can be used to determine the target and contact surfaces. In the rigid-soft contact type, the target surface is a rigid body surface, and the contact surface is a soft body surface. The following rules should be followed in the soft-soft contact type:

- If a convex surface touches a flat or concave surface, the flat or concave surface shall be the target surface;
- If one face has a dense mesh and the other has a coarser mesh, the coarse

mesh should be the contact surface and the coarse mesh should be the target surface;

- If one surface is more rigid than the other, the softer surface is the contact surface and the harder surface is the target surface;
- If the higher-order element is on one outer surface and the lower-order element is on the other surface, the face of the higher-order element is the contact face, and the face of the lower-order element is the target face;
- If one face is significantly larger than the other, the larger face is the target face.

According to the above definition rules for the contact surface and the target surface, analyzing the contact in this paper, when it is an elastic substrate, the interface (substrate) is the contact surface, and the interface (coating) is the target surface; when it is the rigid substrate, the interface (substrate) is the target surface, and the interface (coating) is the contact surface.

2.2. Common Real Constants

Common real constants include contact stiffness (FKN), allowable penetration tolerance (FTOLN), Pinball area size (PINB), initial closure factor (ICONT), contact surface offset (CNOF), and initial allowable penetration range (PMAX and PMIN).

All contact elements adopt penalty stiffness (contact stiffness) to ensure the coordination of the contact interface, and the contact spring produces deformation and satisfies the equilibrium equation.

$$F = k\Delta, \tag{1}$$

where k is the contact stiffness.

Mathematically, in order to maintain balance, the penetration value is needed, but the physical contact entity does not penetrate. The difficult choice for analysis is: the small penetration calculation accuracy is high, so the contact stiffness should be large. However, too large contact stiffness will cause convergence difficulties, the model may oscillate, and the contact surfaces will jump away from each other. Therefore, the contact stiffness is the most important parameter that affects the calculation accuracy and convergence at the same time, and an appropriate contact stiffness must be selected.

In the process of model debugging in this paper, the observation penetration of the whole model is displayed in the actual proportion. If the penetration is too large, increase the contact stiffness and re-analyze. The number of iterations of convergence can be observed. If the number of iterations is too many (or not convergent), then reduce the contact stiffness and re-analyze. At the same time, the contact stiffness is changed to verify the validity of the calculation results, and the range of contact stiffness is adjusted until the results (stress, strain, etc.) do not change obviously. Finally, after many debugging, the contact stiffness of the model is 13.5.

The shear or sliding behavior of two contact bodies can be frictionless or fric-

tionless. When there is no friction, objects are allowed to slide with each other without resistance; when there is friction, there is a shear force (friction) between objects. Friction consumes energy and is path-dependent behavior. In order to obtain high precision, the time step must be very small. Coulomb model is often used in friction setting, and there is additional selection to deal with complex adhesion and shear behavior. The Coulomb method states that the equivalent shearing force F_T between objects cannot exceed part of the positive pressure F_N.

$$F_T \le \mu F_N, \tag{2}$$

where μ is the coefficient of friction.

Once the actual shear force exceeds F_T, the two bodies will slide relative to each other. In this paper, when the finite element model is friction contact, the friction coefficient is 0.3; when the finite element model is smooth contact, the friction coefficient is 0.

3. Interface Connection Form Effect, Substrate Effect

3.1. Loading and Model Settings

Here, the interface connection form effect and substrate effect of the coating structure are analyzed by the control variable method, and the same load $P_z = 8$ is applied to different coating structures (dimensionless, the actual load is divided by c_{33}/h_0^2. c_{33} is the elastic modulus of zinc oxide (ZnO) in **Table 1**, and h_0 is the coating thickness in **Figure 1**). The depth of indentation is deep enough to ensure that the concave surfaces of different coating structures are fully fitted.

The finite element model used in this paper is a two-dimensional axisymmetric simplified model (**Figure 1**). Finite element model **Figure 1** shows the simulation size parameters: substrate (height 15, width 15), coating (thickness $h_0 = 1$, width 15), indenter (inner concave height $h_s = 0.1$, contact radius $a = 3$, bus height 6). The shape of the simulated mesh shown in **Figure 1** of the finite element model: the finite element method is often prone to stress singularity at the tip; So there is a chamfer at the tip of the indenter; the substrate and coating are composed of gradient quadrilateral meshes near the tip of the indenter; The indenter adopts a gradient quadrilateral mesh, and the closer to the tip of the indenter, the greater the density of the indenter, which ensures good convergence and accuracy of calculation. The boundary conditions given in **Figure 1** of the finite element model: the bottom of the substrate is fixed, the left boundary of the coating substrate is axisymmetric horizontal constraint, and the right boundary is free boundary without constraint. The position of the coordinate system given in the local magnification diagram on the left side of the finite element model **Figure 1**: the origin O of the coordinate system is in the lower left corner of the coating, the axis ζ is up and the axis λ is to the right. The performance parameters of the model materials selected for comparison are shown in **Table 1**: hexagonal zinc (Zn) is used in the substrate material and zinc oxide

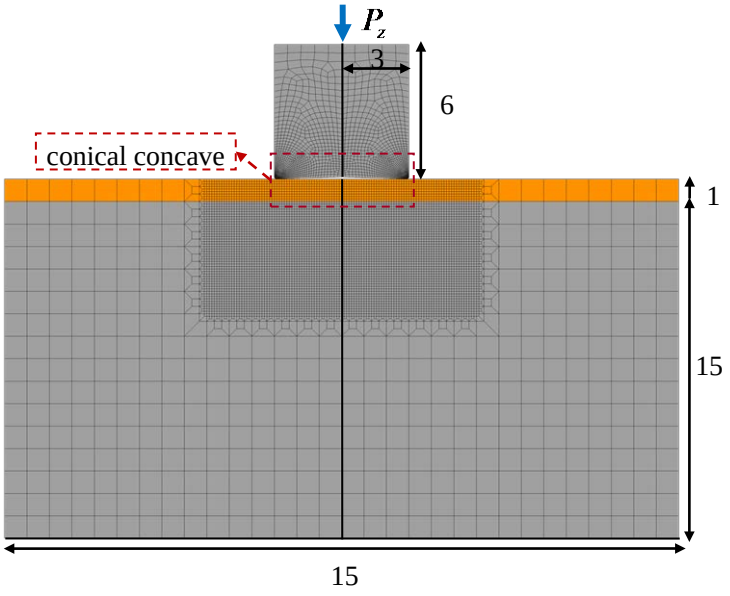

Figure 1. Two-dimensional axisymmetric finite element model.

Table 1. Material properties of coating and substrate.

Elastic modulus (×109 N × m^{-2})	C11	C12	C13	C33	C44
Zinc oxide (ZnO)	209.7	121.1	105.1	210.9	42.5
Hexagonal zinc (Zn)	162.8	50.8	36.2	62.7	38.5

(Zn) is used in the coating material. The elastic modulus of the indenter is much larger than that of the substrate coating (the material properties can be approximately regarded as rigid bodies in the finite element method).

18 finite element models of coating structures analyzed in this section are shown in Table 2. The substrate form is divided into five kinds of elastic substrate (C represents the elastic modulus of the substrate Zn whose coating structure in Table 1 is ZnO/Zn, and 2C represents the elastic modulus of the substrate Zn whose coating structure in Table 1 is twice as large as that of ZnO/Zn substrate, 3C, 4C, 10C, and so on) and rigid substrate (∞C). The interface connection form is divided into Perfect connection (PC), friction contact (FC), smooth contact (SC). An example is given to illustrate that "C_PC" represents that the finite element modulus of the coating structure is elastic substrate I (C), and its interface connection form is Perfect connection (PC). The geometric models of 18 kinds of coating structures are shown in Figure 2. The upper, middle and lower parts of Figure 2 are conical concave indenter, coating and substrate in turn, and 6 substrate forms and 3 interface connection forms are marked with dotted frame on the left (corresponding to Table 2).

3.2. Analysis of the Result of Force Displacement

Figure 3 and Figure 4 are the force and displacement results of 18 finite element models of coating structures shown in Table 2, which reflect the mechanical

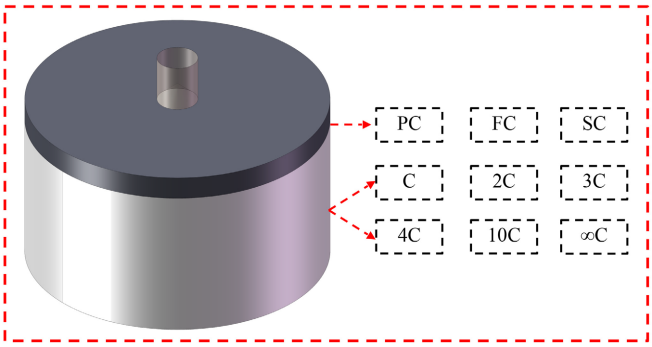

Figure 2. 18 kinds of coating structure geometric model diagram, the combination definition is shown in **Table 2**.

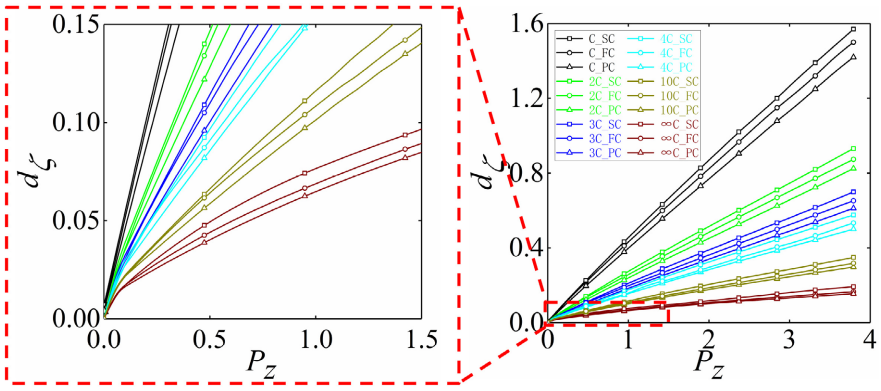

Figure 3. Force displacement result curve of rigid indenter (18 kinds of finite element models of coating structure).

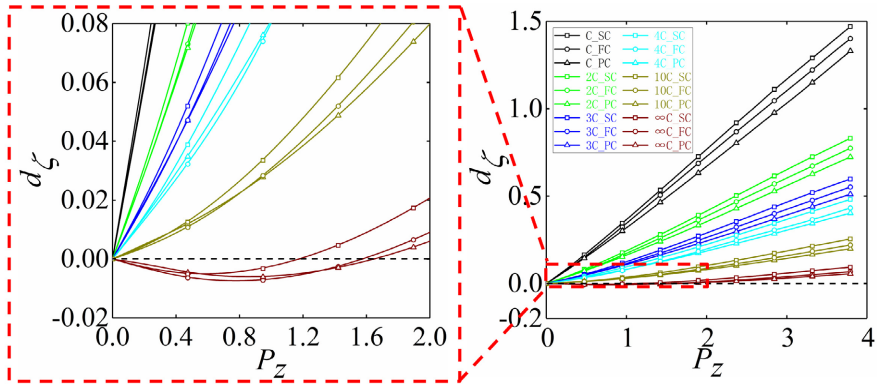

Figure 4. Force displacement curve of the central point of the coating surface (18 finite element models of coating structures).

conditions of different points respectively. **Figure 3** is the result diagram of the force displacement of the rigid head (which can be any point on the rigid head, equivalent to the overall model), and **Figure 4** is the result diagram of the force displacement at the central point of the coating surface. The force and displacement results of 18 kinds of finite element models of coating structures are different by an order of magnitude. In order to show clearly, the red dotted frame in **Figure 3** and **Figure 4** separately draws the local magnified result diagram.

Table 2. 18 finite element models.

Interface connection form		Perfect connection (PC)	Frictional contact (FC)	Smooth contact (SC)
Substrate	Elastic substrate I (C)	C_PC	C_FC	C_SC
	Elastic substrate II (2C)	2C_PC	2C_FC	2C_SC
	Elastic substrate III (3C)	3C_PC	3C_FC	3C_SC
	Elastic substrate VI (4C)	4C_PC	4C_FC	4C_SC
	Elastic substrate V (10C)	10C_PC	10C_FC	10C_SC
	Rigid substrate (∞C)	∞C_PC	∞C_FC	∞C_SC

In **Figure 3**, the force and displacement results of the rigid indenter show that the overall trend of the force and displacement results of the 18 finite element models of coating structures is that the displacement increases with the increase of force. According to the substrate effect, it can be seen that the curve from top to bottom in **Figure 3** is elastic substrate I (C), elastic substrate II (2C), elastic substrate III (3C), elastic substrate VI (4C), elastic substrate V (10C) and rigid substrate (∞C) (under the same load). That is, with the increase of the elastic modulus of the substrate, the coating structure is more difficult to press in. According to the interface connection form, the displacement results of smooth contact (SC) > friction contact (FC) > Perfect connection (PC) (under the same load). That is, the ease of indentation: smooth contact (SC) coating structure > friction contact (FC) coating structure > Perfect connection (PC) coating structure. In **Figure 3**, the force displacement result diagram in the single red dotted frame shows that the force displacement result curve tends to be nonlinear with the increase of elastic modulus, when the elastic modulus is larger or the rigid substrate (∞C). The stiffness is relatively small when the indentation depth is relatively small, and the stiffness increases with the increase of indentation depth, that is, it becomes more and more difficult to indent with the increase of indentation depth.

When the load is the same, in **Figure 4** the force and displacement results of the central point of the coating surface show that the force and displacement results of the finite element models of 18 kinds of coating structures and the force and displacement results of the rigid indenter in **Figure 3** satisfy

$$d_{\varsigma}\ (\textbf{Figure 3}) = d_{\varsigma}\ (\textbf{Figure 4}) + d_{s}, \tag{3}$$

The correctness of **Figure 3** is verified. According to the analysis of the substrate effect and the interface connection form, the conclusion is the same as that of the force displacement curve of the rigid indenter in **Figure 3**. According to the substrate effect, it can be seen that the curve from top to bottom in **Figure 3** is elastic substrate I (C), elastic substrate II (2C), elastic substrate III (3C), elastic substrate VI (4C), elastic substrate V (10C) and rigid substrate (∞C) (under the same load), that is, with the increase of the elastic modulus of the substrate, the coating structure is more difficult to press in. According to the interface connec-

tion form, the displacement results of smooth contact (SC) > friction contact (FC) > Perfect connection (PC) (under the same load), that is, the ease of indentation: smooth contact (SC) coating structure > friction contact (FC) coating structure > Perfect connection (PC) coating structure. The difference is that: in Figure 4 the force displacement result diagram in the separate red dotted frame shows that the central point of the coating surface has a negative displacement at the initial stage of the concave indenter. That is, when the elastic modulus of the substrate approaches the rigid substrate, the motion form of the central point of the coating surface is that the central point of the coating surface will rise upward at the initial stage of the concave indenter, and when the force increases to a certain extent, it moves downward with the indenter.

4. Local Delamination Effect of Interface

The general analysis of the coating structure is the perfect combination of the coating and the substrate at the interface to form a whole coating/substrate structure system, regardless of the influence of interface roughness and adhesion (delamination) on the interface connection [28]. However, in the process of using in high temperature, high speed and extreme environment, the damage of interface delamination will occur due to the poor interface bonding ability, and the good interface bonding between coating and substrate is the basic requirement to ensure the normal use of coating structure. Therefore, it is very important to analyze and study the delamination of the interface. In this chapter, by presupposing that the coating has local delamination at the interface, the finite element models of many kinds of interface local delamination coating structure are calculated and analyzed, and the influence of interface local delamination on the mechanical properties of the coating structure is analyzed. The interfacial stresses of local delaminated coating structure and non-interfacial delaminated coating structure in different regions are compared and analyzed.

4.1. Model and Loading

Here, the same load $P_z = 8$ (dimensionless) is applied to the finite element model of the coating structure in different delamination regions of the elastic substrate I (C) in Table 2, and the indentation depth is deep enough to ensure that the cone concave surface is completely fitted. The mechanical properties of the finite element model of the local delamination coating structure are analyzed. The parameters of the finite element model are shown in Figure 1, and the material parameters used in the finite element simulation also use the ZnO/Zn coating structure system in Table 1. The geometric model of the local delamination coating structure is shown in Figure 5. The upper, middle and lower parts are concave indenter, coating and substrate in turn; the connection form of the interface is shown on the left, and gray-black and gray-white represent joint fixing (PC) and friction contact (FC), respectively, that is, friction contact (FC) region represents local delamination. At the same time, the $O\lambda$ coordinate

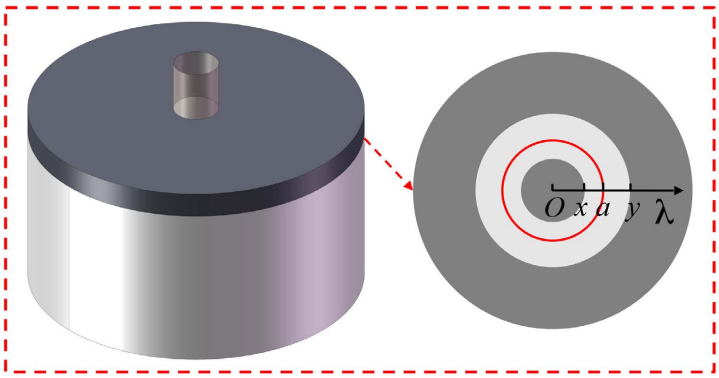

Figure 5. Geometric model diagram of partial delamination coating structure.

system of the delamination region in the substrate region is expressed by *x*-*y*, the *a* in the $O\lambda$ coordinate system is the indenter radius, and the lower part (substrate) is the elastic substrate I (C).

4.2. Comparative Analysis of Interface Stress Results

Figure 6 shows the curve comparison of normal stress σ_ζ and shear stress $\tau_{\xi\zeta}$ of local interface delamination and non-delamination (delamination region 0-0) in 14 different regions. In **Figures 6(a)-(e)**, the local interface delamination size of 5 different regions is all *a* (*a* is the pressure head radius). **Figures 6(f)-(n)** of 9 kinds of different parts of the interface partial separation size are *a*/2.

In **Figure 6**, the horizontal coordinate λ of each picture corresponds to the coordinate position of the interface. The left longitudinal axis is normal stress, and the right longitudinal axis is shear stress; each picture has 6 lines of different colors, marked digital respectively, corresponding to digital with square arrows on the curve; the light red region in each image corresponds to the normal stressc σ_ζ and shear stress $\tau_{\lambda\zeta}$ in the delamination region.

The delamination region $\lambda \in [0,a]$ has the interface local delamination of **Figure 6(a)** & **Figures 6(f)-(h)**. It can be seen that the delamination in region $\lambda \in [0,a]$ has little influence on the normal stress σ_ζ and shear stress $\tau_{\lambda\zeta}$, but the influence on the shear stress $\tau_{\lambda\zeta}$ is greater than that of the normal stress σ_ζ.

In $\lambda \in [a,2a]$, the delamination includes **Figures 6(b)-(d)** & **Figures 6(I)-(m)**. As can be seen from the 8 figures, the delamination in region $\lambda \in [a,2a]$ has a great influence on both normal stress σ_ζ and shear stress $\tau_{\lambda\zeta}$. Similarly, the influence on the shear stress $\tau_{\lambda\zeta}$ is greater than that of the normal stress σ_ζ. The great influence on normal stress σ_ζ and shear stress $\tau_{\lambda\zeta}$ means that the normal stress σ_ζ and shear stress $\tau_{\lambda\zeta}$ in the delamination region (friction contact region) change greatly compared with the non-delamination coating structure in this region, and there is also a great difference between the lower surface of the coating and the upper surface of the substrate, which can easily lead to further delamination of the delamination coating structure.

In the delamination region $\lambda > 2a$, the delamination includes **Figure 6(e)**

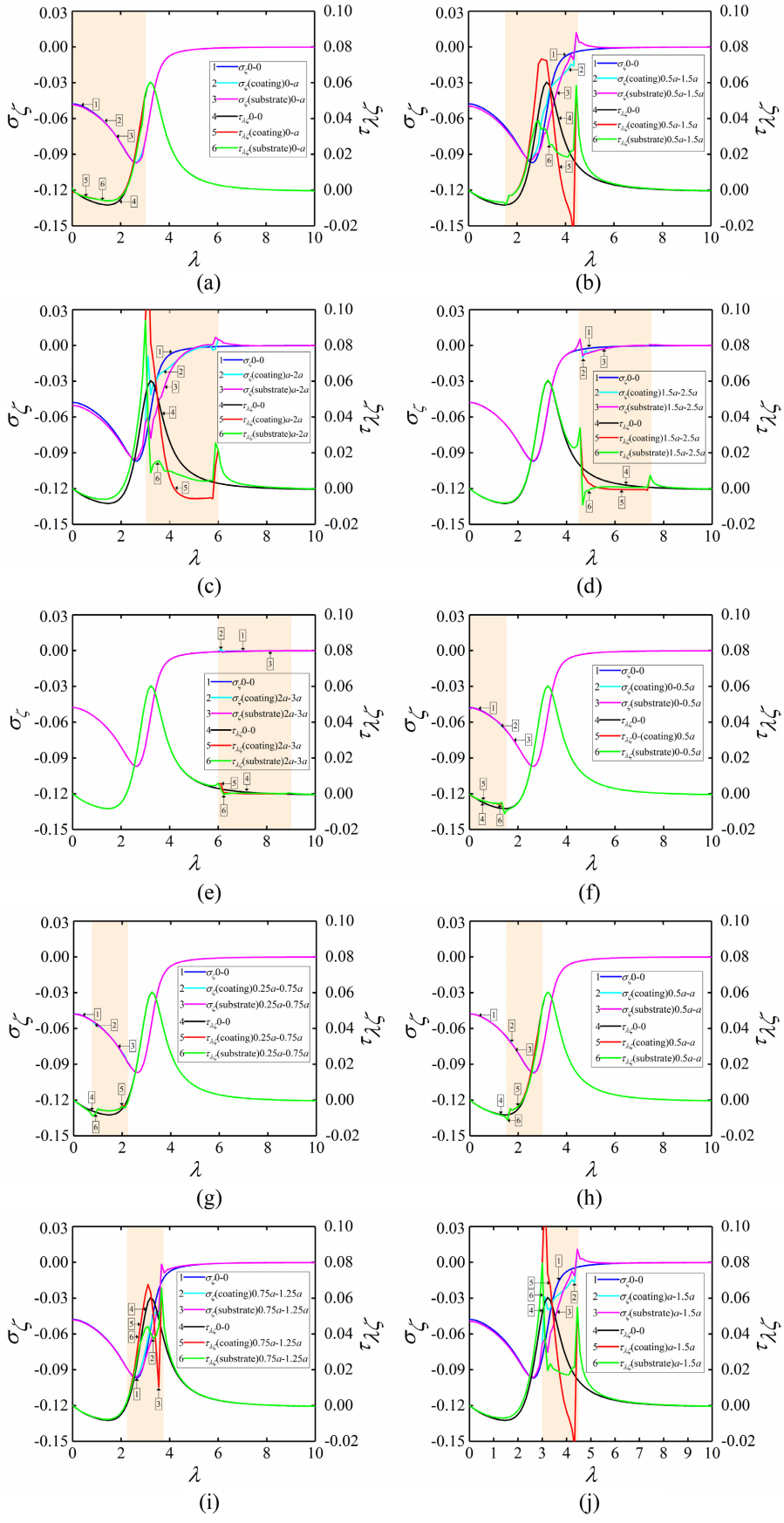
(a)
(b)
(c)
(d)
(e)
(f)
(g)
(h)
(i)
(j)

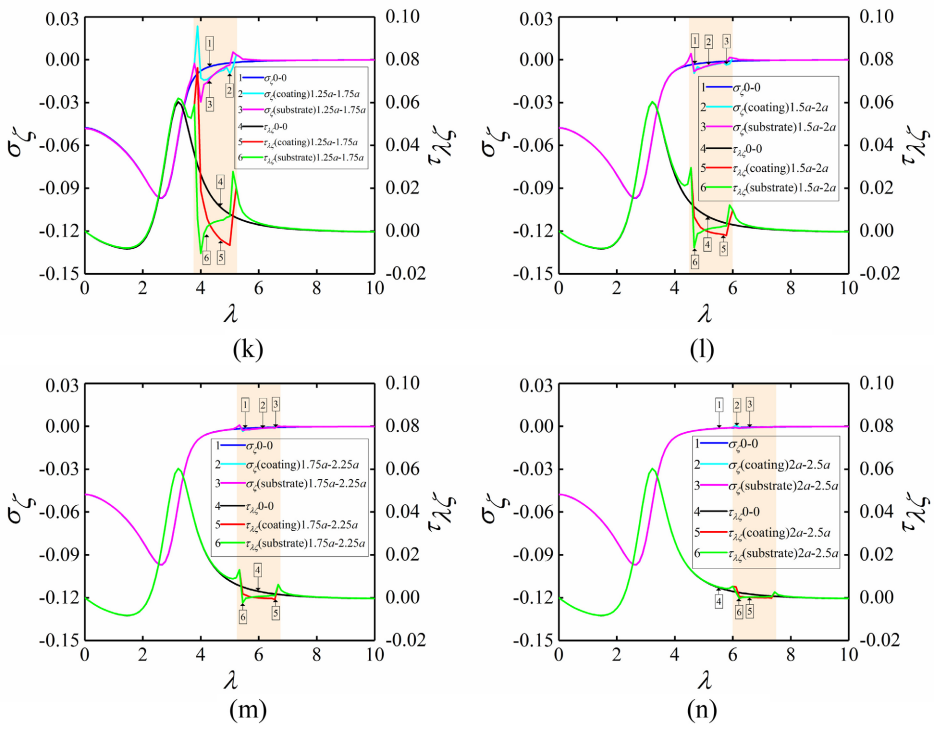

Figure 6. The normal stress σ_ζ and shear stress $\tau_{\xi\zeta}$ curves of local delamination and no delamination (delamination region 0-0): (a) Delamination region 0-*a*; (b) Delamination region 0.5*a*-1.5*a*; (c) Delamination region *a*-2*a*; (d) Delamination region 1.5*a*-2.5*a*; (e) Delamination region 2*a*-3*a*; (f) Delamination region 0-0.5*a*; (g) Delamination region 0.25*a*-0.75*a*; (h) Delamination region 0.5*a*-*a*; (I) Delamination region 0.75*a*-1.25*a*; (j) Delamination region *a*-1.5*a*; (k) Delamination region 1.25*a*-1.75*a*; (l) Delamination region 1.5*a*-2*a*; (m) Delamination region 1.75*a*-2.25*a*; (n) Delamination region 2*a*-2.5*a*.

Figure 6(n). It can be seen in the 2 pictures that the delamination region is the same as the delamination region $\lambda \in [0, a]$. The delamination region $\lambda \in [0, a]$ has less influence on the normal stress σ_ζ and shear stress $\tau_{\lambda\zeta}$. The effect on the shear stress $\tau_{\lambda\zeta}$ is greater than that of the normal stress σ_ζ.

5. Conclusions

In this paper, based on the contact theory of finite element method, three kinds of effects of interface connection, substrate and local delamination on coating structure under the action of the conical concave indenter are analyzed and studied.

For the interface connection form and substrate effects of coating structure: the establishment of contact pair of finite element method is introduced. Different finite element models of coating structure are set up to simulate different interface connection forms and substrate conditions, and the force-displacement is analyzed in detail. According to the analysis of the result, when the friction coefficient is the only variable, the larger the friction coefficient is, the less easy the delamination is, and when the elastic modulus of the substrate is the only variable, the smaller the elastic modulus is , the less easy the delamination is. It is

worth noting that with the change of friction coefficient and elastic modulus, the force-displacement curve is not linear. The smaller the friction coefficient and the larger the elastic modulus, the more obvious the nonlinear characteristic of the force-displacement curve.

For the interface local delamination effect of the coating structure: the interfacial stresses of local delamination coating structure and non-delamination coating structure in different regions are compared and analyzed. We draw a conclusion: the delamination region $\lambda \in [a, 2a]$ has a great influence on both normal stress σ_ζ and shear stress $\tau_{\lambda\zeta}$, and the effect on shear stress $\tau_{\lambda\zeta}$ is greater than that of normal stress σ_ζ.

In this paper, the study of the three effects of coating structure under the action of conical concave indenter is the basis for the study of more complex effects (such as fracture effect) in the future. At the same time, it provides convenience for the future study of the three effects of more complex coating structures: different indenter, multi-layer coating, three-dimensional finite element coating structure and piezoelectric coating structure.

Acknowledgements

The authors thankfully acknowledge the financial support from National Natural Science Foundation of China (NO. 12102143) and the Fundamental Research Funds for the Central Universities (NO. 21621022).

Conflicts of Interest

The authors declare no conflicts of interest regarding the publication of this paper.

References

[1] Chen, F.L., He, X., Prieto-Munoz, P.A. and Yin, H.M. (2015) Opening-Mode Fractures of a Brittle Coating Bonded to an Elasto-Plastic Substrate. *International Journal of Plasticity*, **67**, 171-191. https://doi.org/10.1016/j.ijplas.2014.10.007

[2] Alfano, M., Girolamo, G.D., Pagnotta, L., Zekonyte, J. and Wood, R.J.K. (2011) Depth Sensing Indentation of Oxidized Plasma Sprayed CoNiCrAlY Coatings. *Soft Nanoscience Letters*, **1**, 51-53. https://doi.org/10.4236/snl.2011.12009

[3] Wang, L., Liu, X.H., Li, D.C., Liu, F. and Jin, Z.M. (2014) Contact Mechanics Studies of an Ellipsoidal Contact Bearing Surface of Metal-on-Metal Hip Prostheses under Micro-Lateralization. *Medical Engineering & Physics*, **36**, 419-424. https://doi.org/10.1016/j.medengphy.2013.12.017

[4] Zhuang, J.J., Guo, Y.Q., Xiang, N., Xiong, Y., Hu, Q. and Song, R.G. (2015) A Study on Microstructure and Corrosion Resistance of ZrO_2-Containing PEO Coatings Formed on AZ31 Mg Alloy in Phosphate-Based Electrolyte. *Applied Surface Science*, **357**, 1463-1471. https://doi.org/10.1016/j.apsusc.2015.10.025

[5] Deyab, M.A. (2015) Effect of Carbon Nano-Tubes on the Corrosion Resistance of Alkyd Coating Immersed in Sodium Chloride Solution. *Progress in Organic Coatings*, **85**, 146-150. https://doi.org/10.1016/j.porgcoat.2015.04.003

[6] Shen, W.N., Feng, L.J., Liu, X., Luo, H., Liu, Z., Tong, P.R. and Zhang, W.H. (2016)

Multiwall Carbon Nanotubes-Reinforced Epoxy Hybrid Coatings with High Electrical Conductivity and Corrosion Resistance Prepared via Electrostatic Spraying. *Progress in Organic Coatings*, **90**, 139-146. https://doi.org/10.1016/j.porgcoat.2015.10.006

[7] Guan, X.Y., Wang, Y.X., Xue, Q.J. and Wang, L.P. (2015) Toward High Load Bearing Capacity and Corrosion Resistance Cr/Cr_2N Nano-Multilayer Coatings against Seawater Attack. *Surface & Coatings Technology*, **282**, 78-85. https://doi.org/10.1016/j.surfcoat.2015.10.016

[8] Kumar, U.P., Kennady, C.J. and Zhou, Q.Y. (2015) Effect of Salicylaldehyde on Microstructure and Corrosion Resistance of Electrodeposited Nanocrystalline Ni-W Alloy Coatings. *Surface & Coatings Technology*, **283**, 148-155. https://doi.org/10.1016/j.surfcoat.2015.10.056

[9] Krella, A.K., Sobczyk, A.T., Krupa, A. and Jaworek, A. (2016) Thermal Resistance of Al_2O_3 Coating Produced by Electrostatic Spray Deposition Method. *Mechanics of Materials*, **98**, 120-133. https://doi.org/10.1016/j.mechmat.2016.05.002

[10] Pedraza, F., Rannou, B., Boissonnet, G., Bouchaud, B. and Maache-Rezzoug, Z. (2015) Rheological Behaviour, Synthesis and Performance of Smart Thermal Barrier Coating Systems Based on Hollow Alumina. *Journal of Materials Science Chemical Engineering*, **3**, 17-22. https://doi.org/10.4236/msce.2015.312004

[11] Favache, A., Sacre, C.H., Coulombier, M., Libralesso, L., Guaino, P., Raskin, J.P., Bailly, C., Nysten, B. and Pardoen, T. (2015) Fracture Mechanics Based Analysis of the Scratch Resistance of Thin Brittle Coatings on a Soft Interlayer. *Wear*, **330-331**, 461-468. https://doi.org/10.1016/j.wear.2015.01.081

[12] Putignano, C., Carbone, G. and Dini, D. (2015) Mechanics of Rough Contacts in Elastic and Viscoelastic Thin Layers. *International Journal of Solids and Structures*, **69-70**, 507-517. https://doi.org/10.1016/j.ijsolstr.2015.04.034

[13] Rogowski, B. (2012) A Concave Indenter on a Piezoelectromagneto-Elastic Substrate or a Layer Elastically Supported. *Journal of Strain Analysis for Engineering Design*, **47**, 362-378. https://doi.org/10.1177/0309324712447899

[14] Wu, F., Li, X.Y., Chen, W.Q., Kang, G.Z. and Muller, R. (2018) Indentation on a Transversely Isotropic Half-Space of Multiferroic Composite Medium with a Circular Contact Region. *International Journal of Engineering Science*, **123**, 236-289. https://doi.org/10.1016/j.ijengsci.2017.11.013

[15] Jeong, K.M., Kim, K.W. and Kim, J.H. (2019) Global-Local Finite Element Analysis for Predicting Separation in Cord-Rubber Composites of Radial Truck Tires. *Open Journal of Modelling and Simulation*, **7**, 190-202. https://doi.org/10.4236/ojmsi.2019.74011

[16] Surana, K.S., Shanbhag, R. and Reddy, J.N. (2017) Finite Element Processes Based on GM/WF in Non-Classical Solid Mechanics. *American Journal of Computational Mathematics*, **7**, 321-349. https://doi.org/10.4236/ajcm.2017.73024

[17] Vasiliev, A.S., Volkov, S.S., Sadyrin, E.V. and Aizikovich, S.M. (2020) Simplified Analytical Solution of the Contact Problem on Indentation of a Coated Half-Space by a Conical Punch. *Mathematics*, **8**, Article No. 983. https://doi.org/10.3390/math8060983

[18] Schwarzer, N., Chudoba, T., Billep, D. and Richter, F. (1999) Investigation of Coating Substrate Compounds Using Inclined Spherical Indentation. *Surface and Coatings Technology*, **116-119**, 244-252. https://doi.org/10.1016/S0257-8972(99)00206-6

[19] Huang, X. and Pelegri, A.A. (2007) Finite Element Analysis on Nanoindentation with Friction Contact at the Film/Substrate Interface. *Composites Science and*

Technology, **67**, 1311-1319. https://doi.org/10.1016/j.compscitech.2006.10.005

[20] Peng, P., Liao, G., Shi, T., Tang, Z. and Gao, Y. (2010) Molecular Dynamic Simulations of Nanoindentation in Aluminum Thin Film on Silicon Substrate. *Applied Surface Science*, **256**, 6284-6290. https://doi.org/10.1016/j.apsusc.2010.04.005

[21] Liu, M. and Yang, F. (2012) Finite Element Analysis of the Indentation-Induced Delamination of Bi-Layer Structures. *Journal of Computational and Theoretical Nanoscience*, **9**, 851-858. https://doi.org/10.1166/jctn.2012.2106

[22] Xu, Z.H. and Rowcliffe, D. (2004) Finite Element Analysis of Substrate Effects on Indentation Behaviour of Thin Films. *Thin Solid Films*, **447**-**448**, 399-405. https://doi.org/10.1016/S0040-6090(03)01071-X

[23] Gamonpilas, C. and Busso, E.P. (2004) On the Effect of Substrate Properties on the Indentation Behaviour of Coated Systems. *Materials Science and Engineering*: *A*, **380**, 52-61. https://doi.org/10.1016/j.msea.2004.04.038

[24] Wang, J.S., Zheng, X.J., Zheng, H., Song, S.T. and Zhu, Z. (2010) Identification of Elastic Parameters of Transversely Isotropic Thin Films by Combining Nanoindentation and Fem Analysis. *Computational Materials Science*, **49**, 378-385. https://doi.org/10.1016/j.commatsci.2010.05.025

[25] Abdul-Baqi, A. and Van der Giessen, E. (2001) Indentation-Induced Interface Delamination of a Strong Film on a Ductile Substrate. *Thin Solid Films*, **381**, 143-154. https://doi.org/10.1016/S0040-6090(00)01344-4

[26] Diao, D. and Kandori, A. (2006) Finite Element Analysis of the Effect of Interfacial Roughness and Adhesion Strength on the Local Delamination of Hard Coating under Sliding Contact. *Tribology International*, **39**, 849-855. https://doi.org/10.1016/j.triboint.2005.07.037

[27] Xiao, Y., Shi, W. and Luo, J. (2015) Indentation for Evaluating Cracking and Delamination of Thin Coatings Using Finite Element Analysis. *Vacuum*, **122**, 17-30. https://doi.org/10.1016/j.vacuum.2015.09.003

[28] Wang, Z.J., Shen, X.J., Chen, X.Y. and Zhang, T. (2016) Effects of Coating Material Characteristics on Rolling Bearing Contact Performance. *Transactions of Beijing Institute of Technology*, **36**, 370-375. https://doi.org/10.15918/j.tbit1001-0645.2016.04.007